

Recursive Transmitted Reference Receivers for Impulse Radio UWB Systems

Muhammad Gufran Khan, Jörgen Nordberg

August 27, 2008

Abstract

For the detection of impulse radio (IR) UWB signals, RAKE receivers or transmitted reference (TR) autocorrelation receivers can be used. The complexity of RAKE receiver increases significantly when the number of received multipath components is large. The TR scheme is a low-complexity alternative as it does not require channel estimation. However, there is a performance loss associated with the low-complexity TR scheme. The recursive structures of the conventional TR and averaged TR schemes are presented to improve the detection performance of IR-UWB signals. The performance of proposed schemes is evaluated over the standard IEEE 802.15.4a multipath channels. The performance is compared with conventional TR receivers in terms of uncoded bit-error-rate (BER), assuming that the channel is quasi-static. For averaged and recursive averaged TR schemes, the TR sequence is also slightly modified. The simulation results validate that the proposed schemes have better performance by about 2 dB than the conventional TR and averaged TR receivers.

Chapter 1

Introduction

Ultra-wideband (UWB) radio is emerging worldwide as a particularly appealing transmission technique for applications requiring either high bit rates over short ranges or low bit rates over medium-to-long ranges [1]. The impulse radio UWB offers some unique qualities such as high-resolution, low power spectral density and wide bandwidth which makes them suitable for diverse applications such as wireless personal area networks (WPANs) and wireless sensor networks.

Impulse radio UWB systems utilize very narrow pulses for the transmission. The sub-nanosecond nature of these pulses provides rich multipath diversity at the receiver as a large number of (on the order of hundred) multipath components (MPCs) can be resolved. The multipath diversity available at the receiver can be exploited using a RAKE structure [2]. Since the number of resolved MPCs is very high, a RAKE receiver needs a large number of correlators (fingers) [3]. Providing a receiver with a large number of correlators, however, increases the receiver complexity [4]. Furthermore, a RAKE receiver needs to estimate the channel impulse response in order to obtain the correct RAKE weights [5].

Alternatively, transmitted reference scheme is a sub-optimum autocorrelation receiver scheme for the demodulation of IR-UWB signals [6], [7]. Transmitted reference communication systems operate by transmitting a pair of unmodulated and modulated signals and employing the former to demodulate the latter [7]. Since the reference signal and data signal are transmitted within the coherence time of the channel, it is assumed that the channel responses to the two signals are the same [8]. One drawback of TR scheme is a loss of at least 6 dB compared to an ideal matched filter receiver, 3 dB due to noise contained within the reference pulse and 3 dB due to usage of two pulses per bit, instead of one [9]. Secondly, the performance of TR system is severely limited by the use of noisy unmodulated pulses as templates at the

receiver [12].

In the literature, different transmitted reference schemes have been described with the aim to achieve a low-complexity detection. In [6], an averaged TR (ATR) system which performs averaging of all the reference pulses in a previous symbol interval has been proposed to remedy the problem of noisy reference pulse. However, the suppression of noise by averaging previously received reference pulses requires the implementation of precise delays which may be burdensome [6]. In [8], optimal and suboptimal UWB TR receivers are analyzed and a differential TR system is presented in which no reference pulses are transmitted. However, the differential TR system also suffers from the noisy reference template. A differential TR detector and its iterative solution is also considered and analyzed in [10]. Further, a decision directed autocorrelation receiver and its recursive solution is proposed in [11] for pulsed ultra-wideband systems. The decision directed scheme decreases the signaling overhead but relies on the past symbol decisions.

In this report, a recursive TR (R-TR) and a recursive averaged TR (R-ATR) receiver scheme is investigated and proposed with the aim to improve the performance of the conventional IR-UWB TR schemes. The R-TR structure estimates the reference template for the correlator frame-by-frame recursively from the previous template and the newly received reference pulse. The R-ATR structure estimates the reference template bit-by-bit recursively from the previous template and the average over the reference pulses within current bit. The R-TR receiver has low-complexity as the delays are short and the correlation can be performed in the analog domain avoiding the high sampling requirements. However, the R-ATR receiver requires a single bit long delay element for recursion. The comparison of the proposed receivers has been performed with the conventional TR and ATR receivers. The simulation results validate that the proposed schemes exhibit a performance gain over the conventional TR receivers.

The rest of the report is outlined as follows. In chapter 2, the system model of a typical TR IR-UWB system is described. In Chapter 3, the UWB channel model used for the performance evaluation of the system is discussed. Chapter 4 presents different types of TR receiver structures. The performance evaluation and the results are discussed in Chapter 5 and finally the conclusions are presented in Chapter 6.

Chapter 2

System Model

The transmitted signal of a IR-UWB system using binary antipodal modulation and TR signaling can be written as

$$s(t) = \sqrt{E_p} \sum_{j=-\infty}^{\infty} \left[p(t - jT_f) + b_{\lfloor j/N_f \rfloor} p(t - jT_f - T_d) \right], \quad (2.1)$$

where $p(t)$ is the transmitted normalized UWB pulse of duration T_p i.e., $\int_0^{T_p} [p(t)]^2 dt = 1$, E_p is energy of each pulse, T_f is the frame duration, N_f is the number of frames. Each frame contains two pulses separated by a fixed delay of duration T_d . Moreover, $b_{\lfloor j/N_f \rfloor}$ explains that each bit is transmitted by N_f successive frames. Thus, one binary information symbol $b_{\lfloor j/N_f \rfloor} \in \{1, -1\}$ is transmitted by a stream of $2N_f$ pulses.

In Fig. 2.1, the block diagram of the simplified TR transmitter introduced by Hoyer and Tomlinson [7] is shown. An example of the transmitted sequence for TR and R-TR receiver schemes is shown in Fig. 2.2(a). It shows that the reference pulse is transmitted first and its corresponding data-modulated pulse follows immediately with a delay T_d . Similarly, Fig. 2.2(b) represents the transmitted sequence of pulses which has been slightly modified for ATR and R-ATR receiver schemes. It illustrates that all the reference pulses in a bit interval are transmitted together and their corresponding data-modulated pulses follow with a delay $T_d = N_f T_f / 2$

The signal is further transmitted over a multipath channel. Assuming that the impulse response of the channel is based on tapped delay line model with statistically independent tap weights as

$$h(t) = \sum_{k=0}^{K-1} \alpha_k \delta(t - \tau_k), \quad (2.2)$$

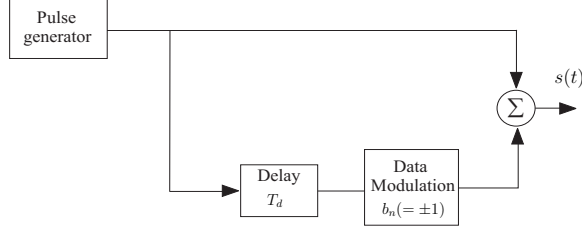


Figure 2.1: Block diagram of the simplified TR transmitter (it can be used for both signaling schemes).

where α_k are the channel tap weights, K is the number of multipath components and τ_k is the delays associated with k th multipath components. The received signal after passing through the multipath channel can be expressed as

$$\begin{aligned}
 r(t) &= \sqrt{E_p} \sum_{j=-\infty}^{\infty} \sum_{k=0}^{K-1} \left[\alpha_k p(t - jT_f - \tau_k) \right. \\
 &\quad \left. + b_{\lfloor j/N_f \rfloor} \alpha_k p(t - jT_f - T_d - \tau_k) \right] + n(t) \\
 &= \sqrt{E_p} \sum_{j=-\infty}^{\infty} \left[g(t - jT_f) \right. \\
 &\quad \left. + b_{\lfloor j/N_f \rfloor} g(t - jT_f - T_d) \right] + n(t), \tag{2.3}
 \end{aligned}$$

where $n(t)$ is a Gaussian process with zero mean and variance σ_n^2 and $g(t)$ is interpreted as the aggregate channel after convolving with the transmitted pulse, $g(t) = p(t) * h(t)$, i.e.,

$$g(t) = \sum_{k=0}^{K-1} \alpha_k p(t - \tau_k), \tag{2.4}$$

The duration of $g(t)$ is defined as $T_g = T_p + T_{m ds}$, where T_p is the pulse duration, $T_{m ds}$ is the maximum delay spread of the channel. In practice, the interference between reference and modulated pulses can be avoided by keeping the delay $T_g \leq T_d$, as shown in Fig. 2.3.

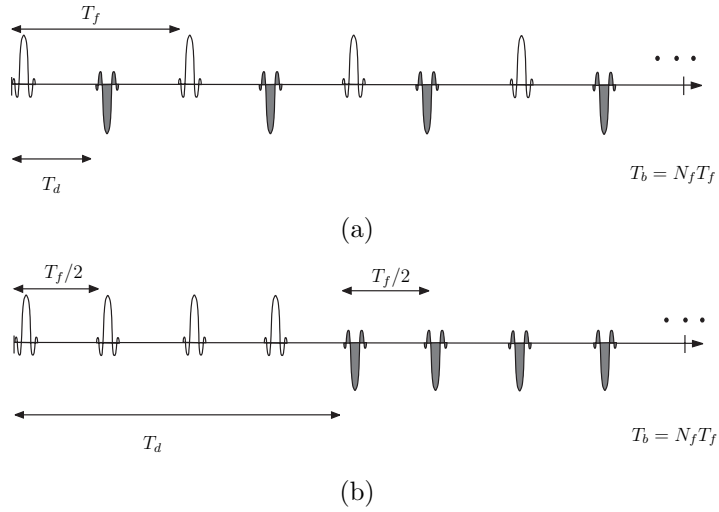


Figure 2.2: An example of the transmitted sequence (a) for TR and R-TR scheme, (b) for ATR and R-ATR scheme, $N_f = 4$ in this figure and the data pulses are shown filled.

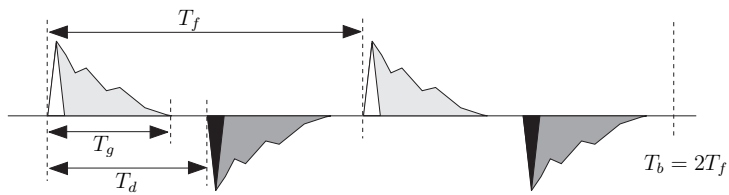


Figure 2.3: An illustration of the aggregate channel after convolving with the transmitted pulse and the delay between the pulses in doublet in TR and R-TR scheme, $N_f = 2$ in this figure.

Chapter 3

UWB Channel

Previously, most of the work has been performed in the area of narrowband channel modeling and characterization, whereas channel modeling for UWB systems is relatively a new area [13]. The narrowband channel models can not be generalized to UWB channels due to some important differences. For example, traditional channel models for path loss assume that diffraction coefficients, attenuation due to materials, and other propagation effects are constant over the band of interest, this assumption is not correct for a UWB system [12]. Further, each multipath component in a UWB system can lead to delay dispersion by itself, due to frequency-selective nature of reflection and diffraction coefficients [13]. In the following section, the UWB channel model used for the evaluation of system performance is discussed briefly.

3.1 UWB Channel Model (IEEE 802.15.4a)

The IEEE 802.15.4a channel model is proposed for sensor networks and similar devices with data rates between 1 kbit/s and several Mbit/s for different office, residential and industrial scenarios. It is a modified version of the Saleh-Valenzuela (SV) model [14] and considers that the multipath components arrive in clusters. The impulse response (in complex baseband) of the general SV model is given as [14],

$$h_{discr}(t) = \sum_{l=0}^{L-1} \sum_{k=0}^{K-1} \alpha_{k,l} e^{j\phi_{k,l}} \delta(t - T_l - \tau_{k,l}), \quad (3.1)$$

where $\alpha_{k,l}$ is the tap weight of the k th component (path) in the l th cluster, T_l is the arrival time of the l th cluster and $\tau_{k,l}$ is the delay of the k th MPC relative to the the l th cluster arrival time T_l . The phases $\phi_{k,l}$ are uniformly distributed, i.e. for a bandpass system, the phase is taken as a uniformly

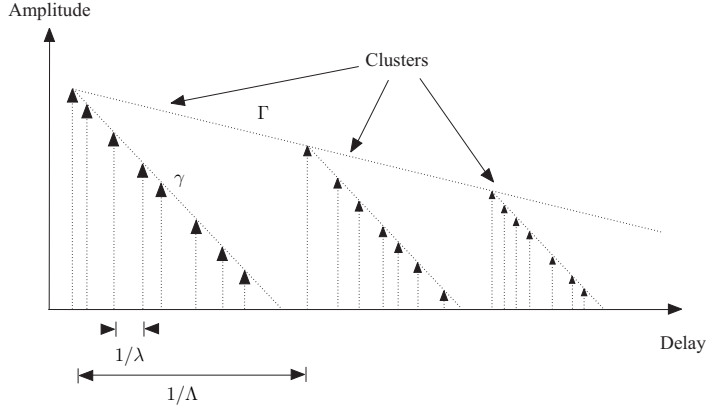


Figure 3.1: Principle of Saleh-Valenzuela model.

random variable in the range from $[0, 2\pi]$ [15]. Fig. 3.1 shows the principle of the SV model, where λ and Λ are ray and cluster arrival rate, respectively, while γ and Γ are ray and cluster decay constants, respectively.

The key features of the IEEE 802.15.4a model as described in [15] are:

- The distribution of cluster arrival times and ray arrival times are given by a Poisson process and a mixture of two Poisson processes, respectively.
- The power delay profile (the mean power of different paths) is exponential within each cluster.
- The cluster decay rates depend linearly on the arrival time of the cluster.
- The distribution for small scale fading statistics is Nakagami- m [15].
- Due to the frequency dependence of propagation effects in a UWB channel, the wideband path loss is a function of frequency as well as of distance.

A complete description of the assumptions and channel model parameters can be found in [15].

Chapter 4

Transmitted Reference Receiver Structures

The transmitted reference (TR) receiver can capture the entire signal energy for a slowly varying channel without requiring channel estimation [6], [12]. Moreover, a potentially attractive feature of UWB autocorrelation receivers is their relative robustness to synchronization problems [7]. However, TR autocorrelation receivers suffers from the use of a noisy received signal as the template for demodulation [12]. In the following sections, the conventional and proposed recursive structures of TR receiver are discussed.

4.1 Transmitted Reference

In a TR receiver, the received signal is passed through a filter which is matched to the transmitted pulse. For simplicity, it is assumed that the shape of the received pulse is the same as the transmitted pulse. However, the propagation and antenna effects may distort the received pulses. The matched filter at the receiver limits the noise in the receiver. The output of the filter is denoted $\tilde{r}(t)$ is given as

$$\tilde{r}(t) = \sqrt{E_p} \sum_{j=-\infty}^{\infty} \left[\tilde{g}(t - jT_f) + b_{\lfloor j/N_f \rfloor} \tilde{g}(t - jT_f - T_d) \right] + \tilde{n}(t), \quad (4.1)$$

where $\tilde{g}(t)$ and $\tilde{n}(t)$ are filtered versions of $g(t)$ and $n(t)$, respectively.

Further, the signal $\tilde{r}(t)$ and a delayed version of this signal are correlated. The outputs of the correlator are summed over the N_f frames to acquire the decision statistic, as shown in Fig. 4.1. The decision statistic for TR signaling [17] can be written as

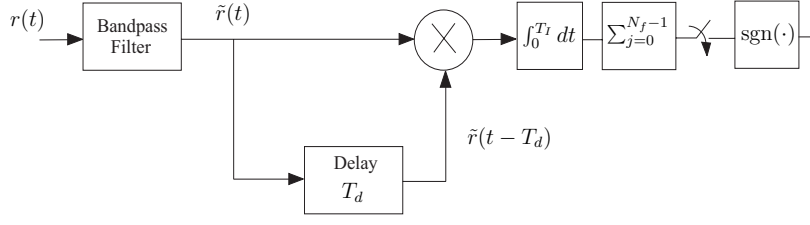


Figure 4.1: Block diagram of the TR receiver.

$$Z_{\text{TR}} = \sum_{j=0}^{N_f-1} \int_{jT_f+T_d}^{jT_f+T_d+T_I} \tilde{r}(t)\tilde{r}(t - T_d)dt, \quad (4.2)$$

where the integration interval T_I in each frame satisfies the assumption $0 < T_I \leq T_g$. The integration interval determines the actual number of multipath components $K_p (\leq K)$ captured by the TR receiver [17]. The auto-correlation process is shown in Fig. 4.2, where the effect of noise is ignored for simplicity [16]. The figure shows that the output of multiplier of the correlator can be divided into signal regions (SRs) and noise-only regions (NORs) [16]. Thus, the choice of integration interval becomes a crucial parameter as the integration should be performed only over the signal regions. It is observed that increasing integration time improves performance up to a certain point, after which the energy capture saturates and only noise is added [12]. It means that the selection of an optimum integration interval can avoid the accumulation of noise in the decision variable.

The bit decision is made using conventional detection as $\hat{b} = \text{sgn}(Z_{\text{TR}})$, where $\text{sgn}(\cdot)$ stands for the sign function. The decision statistic given in (4.2) can also be written as a sum of the terms as

$$Z_{\text{TR}} = Z_1 + Z_2 + Z_3 + Z_4, \quad (4.3)$$

where the terms Z_1 , Z_2 , Z_3 and Z_4 are given by

$$\begin{aligned} Z_1 &= \sum_{j=0}^{N_f-1} \int_{jT_f+T_d}^{jT_f+T_d+T_I} E_p b \tilde{g}(t - jT_f) \tilde{g}(t - jT_f - T_d) dt \\ &= \sum_{j=0}^{N_f-1} \left[\sum_{k=0}^{K_p-1} \alpha_k \int_{jT_f+T_d}^{jT_f+T_d+T_I} E_p b \tilde{p}(t - jT_f - \tau_k) \tilde{p}(t - jT_f - T_d - \tau_k) dt \right], \end{aligned} \quad (4.4)$$

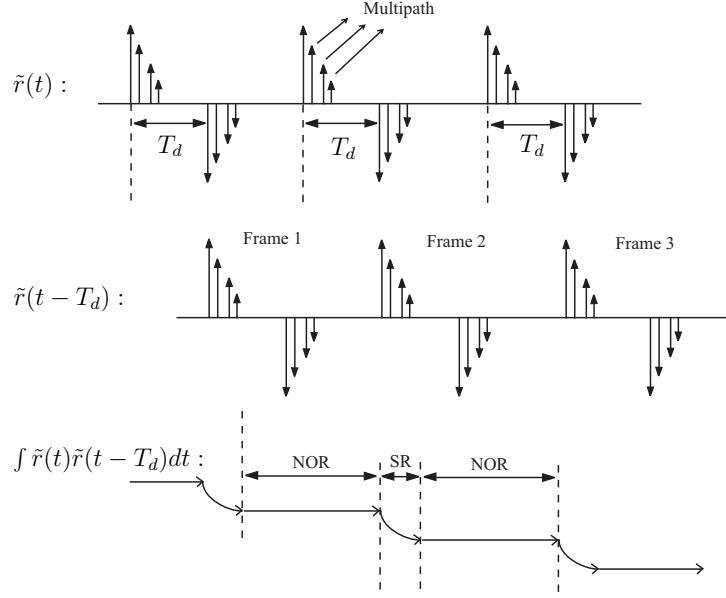


Figure 4.2: An illustration of autocorrelation process of TR receiver, where SR and NOR stand for signal region and noise-only region, respectively, while $N_f = 3$ in the figure [16].

$$\begin{aligned}
Z_2 &= \sum_{j=0}^{N_f-1} \int_{jT_f+T_d}^{jT_f+T_d+T_I} \sqrt{E_p} b \tilde{p}(t - jT_f) \tilde{n}(t - jT_f - T_d) dt \\
&= \sum_{j=0}^{N_f-1} \left[\sum_{k=0}^{K_p-1} \alpha_k \int_{jT_f+T_d}^{jT_f+T_d+T_I} \sqrt{E_p} b \tilde{p}(t - jT_f - \tau_k) \tilde{n}(t - jT_f - T_d) dt \right], \tag{4.5}
\end{aligned}$$

$$\begin{aligned}
Z_3 &= \sum_{j=0}^{N_f-1} \int_{jT_f+T_d}^{jT_f+T_d+T_I} \sqrt{E_p} \tilde{p}(t - jT_f - T_d) \tilde{n}(t - jT_f) dt, \\
&= \sum_{j=0}^{N_f-1} \left[\sum_{k=0}^{K_p-1} \alpha_k \int_{jT_f+T_d}^{jT_f+T_d+T_I} \sqrt{E_p} \tilde{p}(t - jT_f - T_d - \tau_k) \tilde{n}(t - jT_f) dt \right], \tag{4.6}
\end{aligned}$$

$$\begin{aligned}
Z_4 &= \sum_{j=0}^{N_f-1} \int_{jT_f+T_d}^{jT_f+T_d+T_I} \tilde{n}(t-jT_f)\tilde{n}(t-jT_f-T_d)dt \\
&= \sum_{j=0}^{N_f-1} \int_{jT_f+T_d}^{jT_f+T_d+T_I} \tilde{n}(t-jT_f)\tilde{n}(t-jT_f-T_d)dt. \tag{4.7}
\end{aligned}$$

The signal component Z_1 in (4.3) can be approximated as $N_f E_p b \sum_{k=0}^{K_p-1} \alpha_k^2$, where K_p is the number of captured multipath components. The noise is zero mean Gaussian independent of $\tilde{g}(t)$, so the noise-signal terms Z_2 and Z_3 in (4.3) can be considered as zero mean Gaussian random variables. Further, Z_4 is the sum of N_f independent random variables for different values of j . Using the central limit theorem arguments, Z_4 can be modeled as a Gaussian random variable, assuming that time-bandwidth product is large [8]. Hence, the test statistic Z_{TR} is a Gaussian random variable under each channel realization [8], [17]. The conditional mean and variance of decision statistic are given by [17],

$$E(Z_{\text{TR}}|b, \boldsymbol{\alpha}, \boldsymbol{\tau}) = N_f E_p b \sum_{k=0}^{K_p-1} \alpha_k^2. \tag{4.8}$$

$$\text{Var}(Z_{\text{TR}}|\boldsymbol{\alpha}, \boldsymbol{\tau}) = N_f E_p N_o \sum_{k=0}^{K_p-1} \alpha_k^2 + \frac{N_f W T_I N_o^2}{2}. \tag{4.9}$$

Thus, under the Gaussian approximation, the conditional bit error probability (BEP) of TR signaling can be written as [17],

$$\begin{aligned}
P_e|\boldsymbol{\alpha}, \boldsymbol{\tau} &= Q \left(\sqrt{\frac{E[Z_{\text{TR}}|b, \boldsymbol{\alpha}, \boldsymbol{\tau}]^2}{\text{Var}(Z_{\text{TR}}|\boldsymbol{\alpha}, \boldsymbol{\tau})}} \right) \\
&= Q \left(\sqrt{\frac{\left(N_f E_p \sum_{k=0}^{K_p-1} \alpha_k^2 \right)^2}{N_f E_p N_o \sum_{k=0}^{K_p-1} \alpha_k^2 + \frac{N_f W T_I N_o^2}{2}}} \right) \\
&= Q \left(\sqrt{\frac{\left(\frac{N_f E_p}{N_o} \sum_{k=0}^{K_p-1} \alpha_k^2 \right)^2}{\frac{N_f E_p}{N_o} \sum_{k=0}^{K_p-1} \alpha_k^2 + \frac{N_f}{2} W T_I}} \right) \tag{4.10}
\end{aligned}$$

The instantaneous received SNR of TR signaling can be defined as [17],

$$\gamma_{\text{TR}} = \frac{N_f E_p}{N_o} \sum_{k=0}^{K_p-1} \alpha_k^2. \quad (4.11)$$

Then, (4.10) can be written as

$$P_e | \boldsymbol{\alpha}, \boldsymbol{\tau} = Q \left(\sqrt{\frac{\gamma_{\text{TR}}^2}{\gamma_{\text{TR}} + \frac{N_f}{2} W T_I}} \right). \quad (4.12)$$

From (4.11) and (4.12), we see that the amount of received energy captured by the TR receiver depends on the time-bandwidth product, as K_p increases with $W T_I$ [17]. When $K_p = K$, increasing $W T_I$ further only increases the noise in the receiver as shown by the denominator in (4.12) [17].

4.2 Averaged Transmitted Reference

The performance of the TR receiver is limited by the fact that the reference signal used in the correlator is noisy. The performance of TR system can be improved using ATR as shown in Fig. 4.3, which performs averaging over the N_f previous reference pulses prior to demodulation, as described in [6], [8]. This averaging process gives an estimate $\hat{g}(t)$ of the aggregate analog channel $g(t) = p(t) * h(t)$. However, the averaging process is not trivial to perform as it requires long and precise analog delays.

As shown in Fig. 2.2(b), the transmitted sequence is slightly modified for ATR scheme. This signaling sequence needs comparatively shorter delays for averaging and also requires that the channel remains invariant only over one bit duration. Using this signaling sequence, the averaged template denoted as $g_{(\text{ATR})}(t)$ is formed over N_f reference pulses previously received within the current bit duration, as

$$\begin{aligned} g_{(\text{ATR})}(t) &= \frac{1}{N_f} \sum_{i=0}^{N_f-1} \tilde{r}(t + (N_f - i)T_f/2), \\ &= \sqrt{E_p} \tilde{g}(t) + \frac{1}{N_f} \sum_{i=0}^{N_f-1} \tilde{n}(t + (N_f - i)T_f/2). \end{aligned} \quad (4.13)$$

The decision statistic is formed by correlating all the N_f modulated pulses within the current bit duration with the averaged template $g_{(\text{ATR})}(t)$ and can be written as

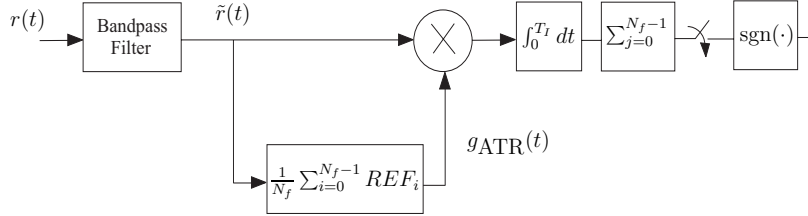


Figure 4.3: Block diagram of the ATR receiver (*REF* stands for the reference pulses).

$$Z_{\text{ATR}} = \sum_{j=0}^{N_f-1} \int_0^{T_I} \tilde{r}(t + jT_f/2) g_{(\text{ATR})}(t) dt. \quad (4.14)$$

4.3 Recursive Transmitted Reference

In the proposed R-TR receiver structure, the reference template is estimated in a recursive manner to enable the receiver to capture adequate multipath diversity, see Fig. 4.4. First, the previous estimated template is obtained using a delay D_f , since the template estimation process assumes that the delay between two subsequent reference pulses is $D_f = T_f$, see Fig. 2.2(a). The previous estimated template and the reference pulse in the newly received frame are pre-multiplied with appropriate weights and then added to obtain new estimated template. Thus, the template update is performed frame-by-frame which essentially requires the weighting and alignment of the previous template estimate and the newly received reference pulse. The complexity of R-TR is less than ATR but more than conventional TR receiver. The recursion process in R-TR receiver structure can be expressed as

$$g_{(\text{R-TR})_k}(t) = \mu g_{(\text{R-TR})_{k-1}}(t - D_f) + \beta \tilde{r}_k(t), \quad t \in [0, T_f/2] \quad (4.15)$$

where $g_{(\text{R-TR})_k}(t)$ is the new template and $g_{(\text{R-TR})_{k-1}}(t - D_f)$ is the previous template estimates at k th and $(k - 1)$ th iteration or frame interval, respectively. The constants μ and β can be considered as the weighting factors of the previous template and the new reference pulse, respectively. These weighting factors can be adjusted as well depending on the channel variations. The constant μ can also be interpreted as the forgetting factor of previous template estimates. If the channel is fast time-varying, this factor can help the estimated template to adapt the channel variations. If the channel is assumed to be static, the parameter $\mu = \beta = 1/2$ can be used, then

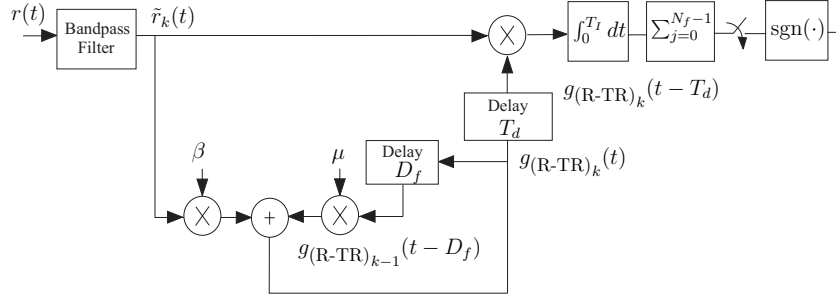


Figure 4.4: Block diagram of the R-TR receiver.

(4.15) reduces to recursive averaging as

$$g_{(\text{R-TR})_k}(t) = \frac{1}{2}[g_{(\text{R-TR})_{k-1}}(t - D_f) + \tilde{r}_k(t)], \quad t \in [0, T_f/2]. \quad (4.16)$$

In this case, the part of the frame which holds the estimated template is the signal region (SR), that is used in the correlation operation. The estimated reference template of R-TR scheme can be written as

$$g_{(\text{R-TR})_j}(t) = \sqrt{E_p} \tilde{g}(t) + \hat{n}_j(t), \quad t \in [0, T_f/2] \quad (4.17)$$

where j stands for the j th template, $\tilde{g}(t)$ is the clean estimated template, and $\hat{n}_j(t)$ is the residual noise in the estimated template. A delayed version of the newly estimated template $g_{(\text{R-TR})_j}(t)$ is obtained by using a delay of T_d , which is the delay between reference and modulated pulse, and correlation is performed with the modulated pulse. In this case, assuming an ideal synchronization, the decision statistic is formed at the output of the correlator after summation over N_f frames and is given by

$$Z_{\text{R-TR}} = \sum_{j=0}^{N_f-1} \int_{jT_f+T_d}^{jT_f+T_d+T_I} \tilde{r}(t) g_{(\text{R-TR})_j}(t - T_d) dt. \quad (4.18)$$

Using (4.17) in (4.18), the decision statistic can be written as

$$\begin{aligned} Z_{\text{R-TR}} = & \sum_{j=0}^{N_f-1} \int_{jT_f+T_d}^{jT_f+T_d+T_I} \left(\sqrt{E_p} b \tilde{g}(t - jT_f) + \tilde{n}(t - jT_f) \right) \\ & \cdot \left(\sqrt{E_p} \tilde{g}(t - jT_f - T_d) + \hat{n}(t - jT_f - T_d) \right) dt, \end{aligned} \quad (4.19)$$

which can be expressed as a sum of the four terms as

$$\begin{aligned}
Z_{\text{R-TR}} &= \sum_{j=0}^{N_f-1} \int_{jT_f+T_d}^{jT_f+T_d+T_I} E_p b \tilde{g}(t - jT_f) \tilde{g}(t - jT_f - T_d) dt \\
&+ \sum_{j=0}^{N_f-1} \int_{jT_f+T_d}^{jT_f+T_d+T_I} \sqrt{E_p} b \tilde{g}(t - jT_f) \hat{n}(t - jT_f - T_d) dt \\
&+ \sum_{j=0}^{N_f-1} \int_{jT_f+T_d}^{jT_f+T_d+T_I} \sqrt{E_p} \tilde{g}(t - jT_f - T_d) \tilde{n}(t - jT_f) dt \\
&+ \sum_{j=0}^{N_f-1} \int_{jT_f+T_d}^{jT_f+T_d+T_I} \tilde{n}(t - jT_f) \hat{n}(t - jT_f - T_d) dt. \quad (4.20)
\end{aligned}$$

The first term is signal term, while second and third terms are independent Gaussian distributed signal-noise terms. As in [8], the fourth, noise-noise term is sum of N_f independent random variables for different values of j . For R-TR receiver, the bit decision is also made using conventional detection as $\hat{b} = \text{sgn}(Z_{\text{R-TR}})$.

4.4 Recursive Averaged Transmitted Reference

The conventional ATR scheme is extended to generate a recursive structure called recursive averaged TR (R-ATR) scheme, as depicted in Fig. 4.5. Like ATR, a slightly modified transmitted sequence shown in Fig. 2.2(b) is used for R-ATR scheme. First, like ATR, the proposed R-ATR receiver performs average by appropriately delaying N_f received reference pulses within the current bit. Further, the resulting averaged waveform and the previously estimated template are pre-multiplied with appropriate weights and added to obtain the new reference template. The previous template estimate is kept in a memory with delay $D_b = N_f T_f$ to be utilized in the recursion process. It is noteworthy that the template update is performed bit-by-bit in this case, which means that there is a slight increase in complexity as compared to ATR.

In a similar fashion as (4.15), the template estimation process can be expressed as

$$g_{(\text{R-ATR})_k}(t) = \mu g_{(\text{R-ATR})_{k-1}}(t - D_b) + \beta g_{(\text{ATR})_k}(t), \quad t \in [0, T_f/2] \quad (4.21)$$

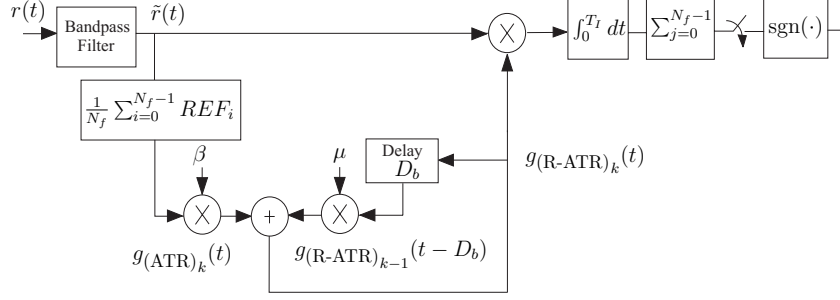


Figure 4.5: Block diagram of the R-ATR receiver (*REF* stands for the reference pulses).

where $g_{(\text{R-ATR})_k}(t)$ is the new template and $g_{(\text{R-ATR})_{k-1}}(t - D_b)$ is the previous template estimates at k th and $(k - 1)$ th iteration or bit interval, respectively. The term $g_{(\text{ATR})_k}(t)$ represents the average over N_f received reference pulses within the current bit duration. Again, the parameter $\mu = \beta = 1/2$ can be used assuming that the channel is static, then (4.21) reduces to recursive averaging as

$$g_{(\text{R-ATR})_k}(t) = \frac{1}{2}[g_{(\text{R-ATR})_{k-1}}(t - D_b) + g_{(\text{ATR})_k}(t)], \quad t \in [0, T_f/2]. \quad (4.22)$$

In case of R-ATR scheme, the newly estimated template $g_{(\text{R-ATR})}(t)$ is used in the correlator for demodulation of all the subsequent N_f data-modulated pulses over a bit interval to form the decision statistic, as

$$Z_{\text{R-ATR}} = \sum_{j=0}^{N_f-1} \int_0^{T_I} \tilde{r}(t + jT_f/2) g_{(\text{R-ATR})}(t) dt. \quad (4.23)$$

4.5 Time-hopping in recursive schemes

The IR-UWB systems use time-hopping (TH) and polarity scrambling to obtain processing gain, to combat multipleaccess interference (MAI), and to smooth the signal spectrum [18]. The recursive schemes described above assume that TH is absent. If TH is used in conjunction with TR signaling, averaging of the template estimates in the R-TR scheme should be performed by appropriately delaying the estimated template from the previous frame using the TH sequence. It requires multiple delay elements, however, the delays are relatively short i.e., on the order of a frame duration. The complexity of the proposed R-ATR scheme can be reduced by repeating the TH sequence

after a bit duration. The recursion process in R-ATR scheme requires only a fixed bit long delay element in this case. The pulse-based polarity scrambling, which can be easily undone at the the receiver [18], can also be used with the recursive schemes.

Chapter 5

Performance Evaluation

In order to evaluate performance of the receivers, TR IR-UWB system is simulated on the multipath channels proposed by IEEE 802.15.4a for low-data-rate UWB systems. The binary antipodal modulation is used employing second derivative of the Gaussian pulse with about 1.4 ns pulse duration. The uncoded data rate of 0.5 Mbps is achieved with $N_f = 10$ and $T_f = 200$ ns. The delay $T_d = 100$ ns and the integration interval within each frame is $T_I = 50$ ns. The channel model CM1 is used which covers residential line-of-sight (LOS) environments with maximum delay spread of about 100 ns, which means that a negligible IFI occurs. The realistic indoor UWB channels usually have long channel coherence time, so the channel coherence time for the channel is assumed to be 0.2 ms and the parameters of the recursive averaging process are set as $\mu = \beta = 1/2$. The energy of the channel impulse responses is normalized as $\sum \alpha_l^2 = 1$ and the system is assumed to be perfectly synchronized.

The simulated uncoded BER curves are shown in Fig. 5.1 for TR and R-TR receiver. The results validate that the R-TR structure has about 2 dB better performance than the conventional TR receiver. It is worth mentioning that in high SNR region, the effect of multipath is more dominant, so increasing the length of the integration interval is more effective to improve the BER. Similarly, Fig. 5.2 shows BER comparison curves for ATR and R-ATR approaches employing the same parameters. The BER plots depict that the R-ATR yields a similar gain in SNR over its simple averaging counterpart, ATR receiver. It can be concluded that the recursive averaging process helps to further alleviate the noise effect in the estimated template, which in turn improves BER performance.

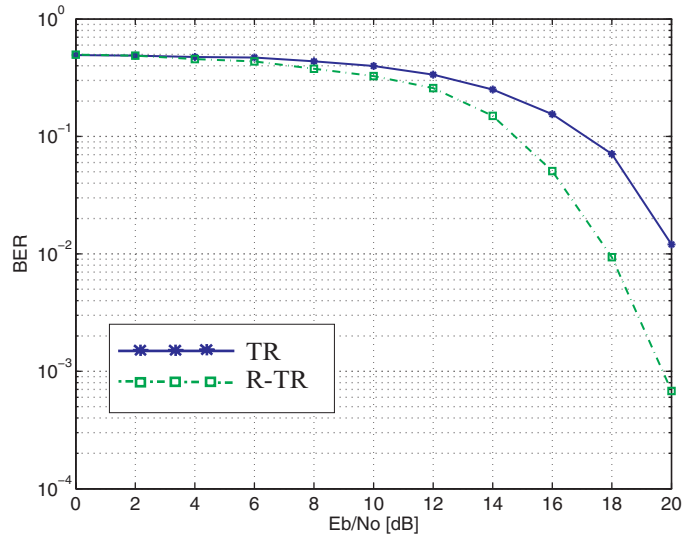


Figure 5.1: Uncoded BER curves of TR and R-TR receivers over CM1 channel.

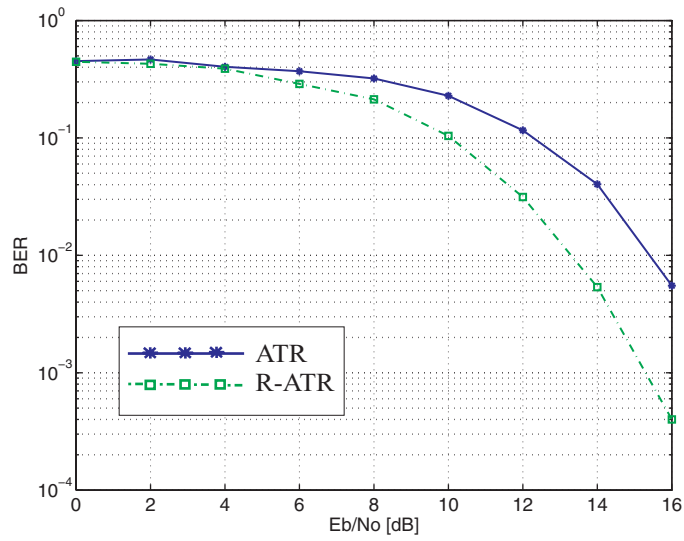


Figure 5.2: Uncoded BER curves of ATR and R-ATR receivers over CM1 channel.

Chapter 6

Conclusions

The recursive schemes of the transmitted reference receiver structure for the detection of impulse radio UWB signals are presented. The proposed recursive schemes estimate the reference template for the correlator recursively by appropriately weighting and aligning the received reference pulses and the previous estimated templates. The proposed R-TR receiver has low-complexity as it requires relatively shorter delays for recursive averaging. Moreover, the use of slightly modified TR signaling sequence in conjunction with ATR and R-ATR receiver scheme is especially of interest as it also requires shorter delays for averaging. In case of time-hopping, the complexity of the recursion process in R-ATR scheme can be reduced by repeating the time-hopping sequence after a bit duration to use a bit long fixed delay. The performance evaluation of the TR IR-UWB system indicates that the R-TR and R-ATR receiver schemes outperform the conventional TR and ATR receiver over slowly-varying channels.

Bibliography

- [1] M.-G. di Benedetto, T. Kaiser and N. Schmidt *UWB – State of the Art*, Journal of Applied Signal Processing Editorial, EURASIP publishing, March 2005.
- [2] J. G. Proakis *Digital Communications*, 4th ed. Boston: McGraw-Hill, 2001.
- [3] M. G. Khan, J. Nordberg, A. Mohammed, and I. Claesson, “Performance evaluation of RAKE receiver for UWB systems using measured channels in industrial environments,” *AusWireless’06, Int. Conf. on Wireless Broadband and Ultrawideband Systems*, March 2006.
- [4] D. Cassioli, M. Z. Win, F. Vatalaro, and A. F. Molisch, “Performance of low-complexity Rake reception in a realistic UWB channel,” *Proc. IEEE ICC’03*, vol.2, pp.763-767, 2003.
- [5] F. Tufvesson and A. F. Molisch, “Ultra-wideband communication using hybrid matched filter correlation receivers,” *Proc. IEEE Veh. Technol. Conf.*, vol. 3, pp. 1290-1294, May 2004.
- [6] D. J. Choi and W. E. Stark “Performance of ultra-wideband communications with suboptimal receivers in multipath channels,” *IEEE Journal of Selected Areas Communications*, vol. 20, no. 9, Dec. 2002, 1754-1766.
- [7] R. T. Hoctor and H. W. Tomlinson, “An overview of delay-hopped, transmitted-reference RF communications,” in *Technical Information Series*: G.E. Research and Development Center, Jan. 2002, pp. 129.
- [8] Y.-L. Chao and R. A. Scholtz “Optimal and suboptimal receivers for ultra-wideband transmitted reference systems,” *IEEE Global Telecommunications Conf. ’03*, vol. 2, pp. 759-763, 1-5 Dec. 2003
- [9] J. Romme and K. Witrisal, “Transmitted-reference UWB systems using weighted autocorrelation receivers,” *IEEE Trans. on Microwave Theory and Tech.*, vol. 54, no. 4, pp. 1754-1761, April 2006.

- [10] G. Durisi and S. Benedetto, "Comparison between coherent and non-coherent receivers for UWB Communications," *UWB – State of the Art*, Journal of Applied Signal Processing Editorial, EURASIP
- [11] S. Zhao, H. Liu, and Z. Tian, "Decision directed autocorrelation receivers for pulsed ultra-wideband systems," *IEEE Trans. Wireless Communications*, vol. 5, no. 8, pp. 2175-2184, Aug. 2006.
- [12] J. H. Reed et. al. *An Introduction to Ultra Wideband Communication Systems*, Prentice Hall, 2005.
- [13] A. F. Molisch *UWB Propagation Channels*, Book chapter 1, pp.1, 2005
- [14] A. Saleh and R. Valenzuela, "A statistical model for indoor multipath propagation," *IEEE Journal on Select. Areas in Communications*, vol. SAC-5, no. 2, pp. 128-137, Feb. 1987.
- [15] A. F. Molisch et al., "IEEE 802.15.4a channel model - final report," Tech. Rep. Document IEEE 802.15-04-0662-02-004a, 2005.
- [16] N. He and C. Tepedelenlioglu, "Performance analysis of non-coherent UWB receivers at different synchronization levels," *Proc. IEEE Globecom*, pp. 3517-3521, 2004.
- [17] T. Q. S. Quek and M. Z. Win, "Analysis of UWB transmitted-reference communication systems in dense multipath channels," *IEEE Journal on Select. Areas in Communications* vol. 23, no. 9, September 2005.
- [18] S. Zhao, P. Orlik, A. F. Molisch, H. Liu, and J. Zhang "Hybrid Ultra-wideband Modulations Compatible for Both Coherent and Transmit-Reference Receivers," *IEEE Trans. on Wireless Communications*.